

Varactor Tuned Ring Resonator Filter With Wide Tunable Bandwidth

Chan Ho Kim¹, Kai Chang², and Xiaoguang Liu¹

¹Dept. of Electrical and Computer Engineering, University of California, Davis, CA 95616, USA

²Dept. of Electrical and Computer Engineering, Texas A&M University, TX 77843, USA

Abstract — This paper presents a ring resonator bandpass filter (BPF) with tunable passband bandwidth. By varying capacitance of four varactors, mid-upper passband bandwidth can be tuned while mid-lower one is almost fixed. An open stub attached to the ring is designed by using an equivalent serial capacitor, and feed lines are designed by analyzing susceptance slope and return losses. Measured results show that the 3dB-fractional bandwidth (FBW) ranges from 70.1 – 85.3 % with the return loss better than 10.9 dB within the passband.

Index Terms — Microstrip filters, ring resonators, stepped impedance stub, tunable filters, varactors.

I. INTRODUCTION

Tunable filters have received much attention from both academia and industry because they can have numerous applications in wireless communication systems. A ring resonator is one of the promising microwave components for implementing diverse tunable filters. Recently, the ring resonators are integrated with tunable J-inverters [1], used as a high-Q two-pole filter fabricated in stripline substrate [2], and used in forced-mode with two loading capacitors [3] to achieve bandwidth or frequency tuning.

In this paper, a ring resonator BPF with a center frequency (f_c) of 2.5 GHz is designed to have tunable bandwidth for the mid-upper passband bandwidth. Four shunt varactors are used for tuning the bandwidth. The proposed BPF herein uses an RT/Duroid 6006 substrate with a thickness of 0.635 mm and a relative dielectric constant $\epsilon_r = 6.15$. EM simulations in this paper are carried out by Ansys HFSS.

II. TUNABLE BPF DESIGN

Fig. 1 shows the configuration of a ring resonator possessing a stepped-impedance stub fed by interdigital-coupled lines. In this figure, Z is the characteristic impedance, and θ is the electrical length. The physical lengths or widths are denoted by l or w in this figure, respectively. Four shunt varactors with capacitance C_V are connected to each via ground. For the simple frequency analysis following, the open stub with the size of $w_2 \times l_2$ is replaced to a serial shorted capacitor with capacitance C_S when $\theta_2 < 90^\circ$. Divided by symmetrical plane, the circuit can be shown as the even- and odd-mode equivalent circuits in Figs. 2(a) and (b), respectively. From these figures, the even- and odd-mode resonance frequencies can be calculated by setting $Y_{in} = 0$, which are expressed by

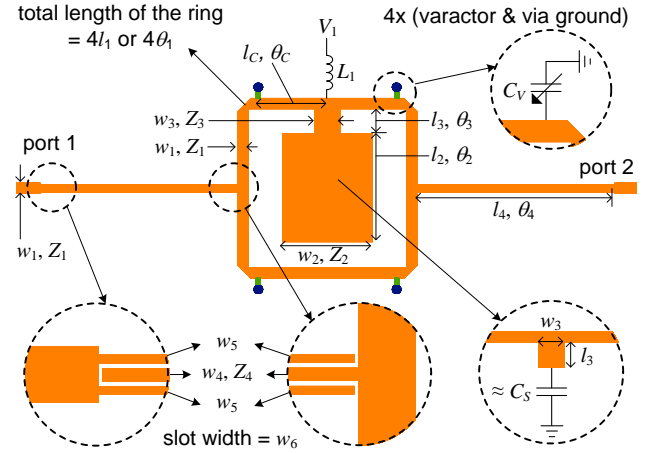


Fig. 1. Schematic of the ring resonator BPF with a stepped-impedance stub and four varactors. The open stub with Z_2 can be replaced with a serial shorted capacitor.

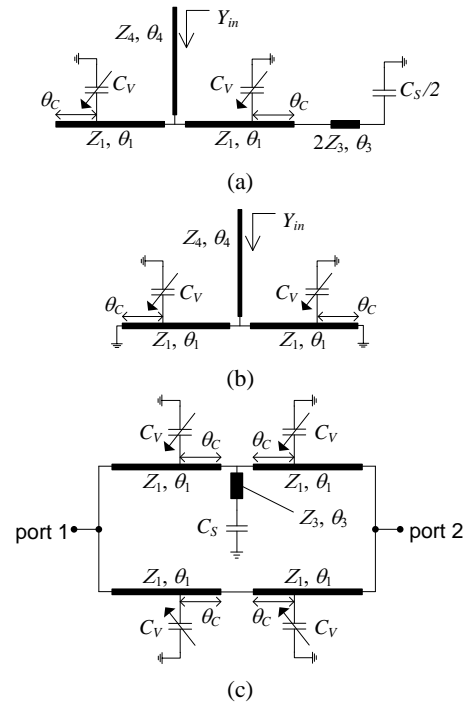


Fig. 2. Equivalent circuit of the ring resonator. (a) Even-mode. (b) Odd-mode. (c) Circuit for calculating transmission zero frequencies.

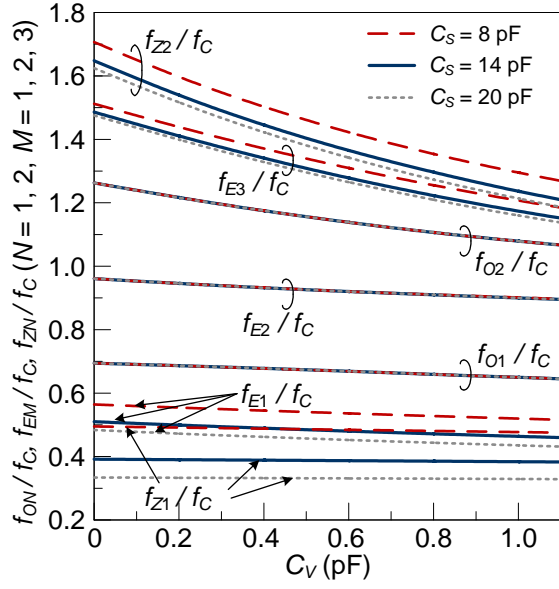


Fig. 3. Resonant frequencies (f_E : even-mode, f_O : odd-mode) and transmission zeros (f_Z) normalized by center frequency (f_C) for the ring resonator when $\theta_3/\theta_1 = 2.2/14$, $\theta_4/\theta_1 = 15.4/14$, $\theta_C/\theta_1 = 7/14$, $Z_1 = 50.1 \Omega$, $Z_3 = 28.8 \Omega$, and $Z_4 = 106.4 \Omega$ ($w_4 = 0.13$ mm).

$$E_1 - \tan \theta_4 / Z_4 + E_2 = 0 \quad \text{for even modes} \quad (1)$$

where

$$E_1 = \frac{\tan(\theta_1 - \theta_C) / Z_1 + \left(2\pi f_E C_V + \frac{\tan \theta_C / Z_1 + E_3}{1 - E_3 Z_1 \tan \theta_C} \right)}{Z_1 \tan(\theta_1 - \theta_C) \left(2\pi f_E C_V + \frac{\tan \theta_C / Z_1 + E_3}{1 - E_3 Z_1 \tan \theta_C} \right) - 1}$$

$$E_2 = \frac{\tan \theta_C / Z_1 + \tan(\theta_1 - \theta_C) / Z_1 + 2\pi f_E C_V}{Z_1 \tan(\theta_1 - \theta_C) (\tan \theta_C / Z_1 + 2\pi f_E C_V) - 1}$$

$$E_3 = \frac{(\tan \theta_3 / 2Z_3 + \pi f_E C_S)}{1 - 2\pi f_E C_S Z_3 \tan \theta_3}$$

and

$$\tan \theta_4 / Z_4 + 2O_1 / O_2 = 0 \quad \text{for odd modes} \quad (2)$$

where

$$O_1 = \tan(\theta_1 - \theta_C) / Z_1 - \cot \theta_C / Z_1 + 2\pi f_{\text{odd}} C_V$$

$$O_2 = Z_1 \tan(\theta_1 - \theta_C) (\cot \theta_C / Z_1 - 2\pi f_{\text{odd}} C_V) + 1.$$

The transmission zero frequencies are obtained when $Y_{21} = Y_{12} = 0$, and Fig. 2(c) is used for calculating these transmission zeros. The equations for these transmission zeros are omitted in this paper for simplicity. Fig. 3 shows three even-mode resonant frequencies (f_{E1} , f_{E2} , f_{E3}), two odd-mode resonant frequencies (f_{O1} , f_{O2}), and two transmission zeros (f_{Z1} , f_{Z2}) normalized by the center frequency (f_C). Both $Z_3 = 28.8 \Omega$ and $\theta_3/\theta_1 = 2.2/14$ are chosen for realizing wide bandwidth [4], and both θ_4 and Z_4 are initially set for the sharp stub of w_4 to have the length of $\lambda_g/4$ at f_C . Also, θ_C is initially set as half θ_1 .

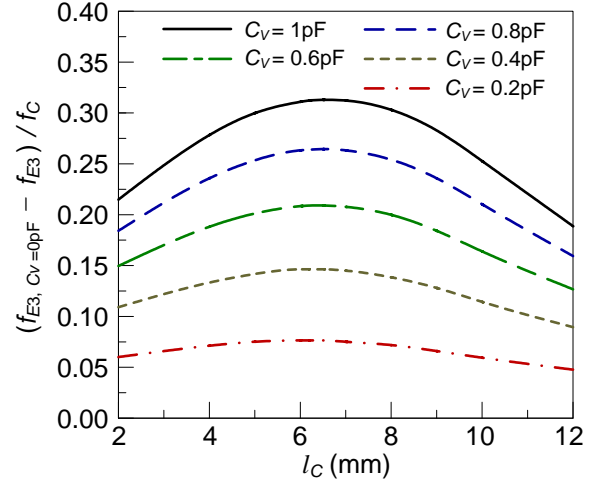


Fig. 4. Tuning level of the ring resonator BPF while the location of varactors (l_C) varies when $\theta_3/\theta_1 = 2.2/14$, $\theta_4/\theta_1 = 15.4/14$, $Z_1 = 50.1 \Omega$, $Z_3 = 28.8 \Omega$, $Z_4 = 106.4 \Omega$ ($w_4 = 0.13$ mm), and $C_S = 14$ pF.

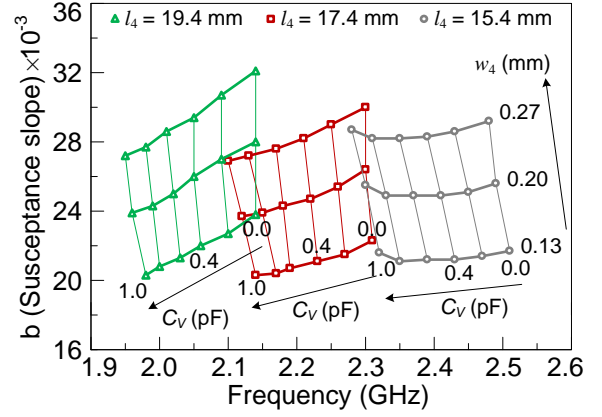


Fig. 5. Susceptance slope b for f_{E2} looking from the end of l_4 . ($l_1 = 14$ mm, $l_3 = 2.2$ mm, $l_C = 6$ mm, $Z_1 = 50.1 \Omega$, $Z_3 = 28.8 \Omega$, $C_S = 14$ pF.)

In particular, f_{Z2} , f_{E3} , and f_{O2} move down significantly to the lower frequencies while C_V increases.

A five pole ($n = 5$) Chebyshev BPF with the FBW of 90% is designed with $f_C = 2.5$ GHz. By using wideband filter transformation equation [5], expressed as

$$\frac{\Omega_K}{\Omega_C} = \frac{2}{\text{FBW}} \left(\frac{f}{f_C} - 1 \right), \quad \Omega_K = \cos \left[\frac{(2k-1)\pi}{10} \right] \quad \text{for } k = 1, 2, \dots, 5 \quad (3)$$

where $\Omega_C = 1$ and $\Omega_K = 0.951, 0.588, 0, -0.588, -0.951$, the normalized frequency (f/f_C) can be calculated as 1.428, 1.265, 1, 0.735, 0.572. Accordingly, the appropriate value for C_S can be chosen in Fig. 3 as 14 pF by comparing the calculated values with the normalized frequencies for $C_V = 0$. This value of C_S is used to realize the open stub with $w_2 \times l_2$.

In order to determine l_C , the tuning level, which is defined by the difference between the normalized f_{E3} for a particular C_V and that for $C_V = 0$, expressed as

$$\text{Tuning level} = \left(f_{E3, C_V=0\text{pF}} - f_{E3} \right) / f_C, \quad (4)$$

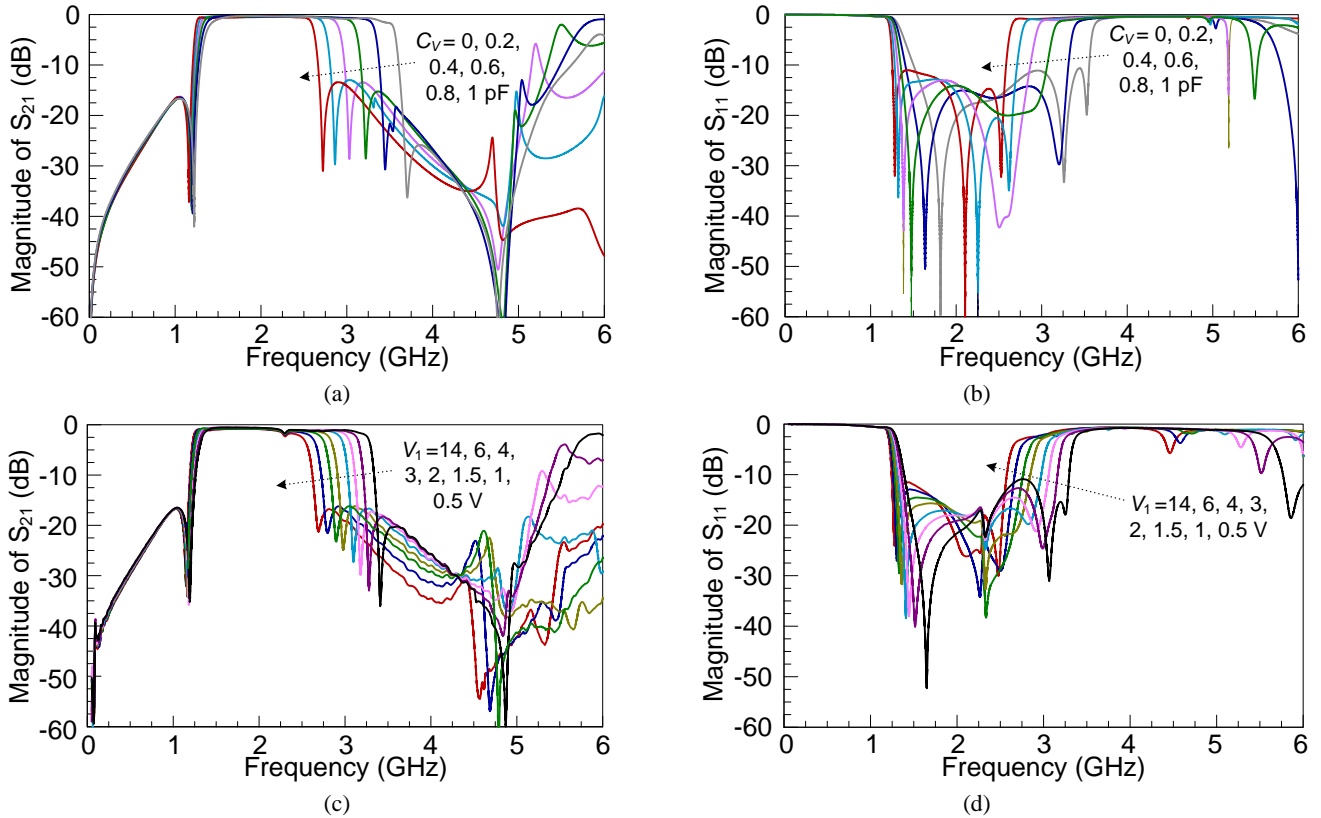


Fig. 6. Results of (a) simulated S_{21} , (b) simulated S_{11} , (c) measured S_{21} and (d) measured S_{11} when C_V and V_1 vary for simulations and measurements, respectively, and $L_1 = 390$ nH. ($l_1 = 14$, $l_2 = 9.5$, $l_3 = 2.2$, $l_4 = 17.4$, $l_c = 6.1$, $w_1 = 0.91$, $w_2 = 7.9$, $w_3 = 2.2$, $w_4 = 0.2$, $w_5 = 0.12$, $w_6 = 0.1$, all in millimeters.)

is examined in Fig. 4. At about 6 mm of l_c , tuning levels are observed to have the highest value. The design for w_4 and l_4 is determined in Fig. 5, which shows the susceptance slope b for f_{E2} looking from the end of l_4 . By considering both the frequency range of f_{E2} and b of the interdigital-coupled feeders while C_V varies, w_4 and l_4 are decided as 0.2 mm and 17.4 mm, respectively.

III. SIMULATED & MEASURED RESULTS

The simulated and measured results are shown in Fig. 6. In the measured results of Figs. 6(c) and (d), bias voltage V_1 varies to change C_V . The higher C_V or lower V_1 makes the narrower bandwidth progressively. Measured and simulated FBWs are 70.1 – 85.3 % and 71.8 – 88.8 % with the return losses better than 10.9 dB and 10.6 dB in the passband, respectively. Measured insertion loss is as low as 0.54 dB, and some notches are observed at approximately 2.3 GHz in Fig. 6(c). These notches are presumed to be due to the fabrication errors on the interdigital-coupled lines, which could act as an open stub with a quarter wavelength at about 2.3 GHz.

IV. CONCLUSION

A wideband BPF with asymmetrically tunable bandwidth has been developed by using a ring resonator consisting of a

stepped-impedance stub and four varactors. The proposed BPF shows good agreement between simulated and measured results, and it shows high tunability for mid-upper bandwidth, high rejection rate at cutoff frequencies, and low insertion losses.

REFERENCES

- [1] K. Kawai, H. Okazaki, and S. Narahashi, "Center frequency, bandwidth, and transfer function tunable bandpass filter using ring resonator and J-inverter," in *Proc. 39th European Microw. Conf.*, 2009, pp. 1207-1210.
- [2] C.-C. Cheng and G. M. Rebeiz, "High-Q 4–6-GHz suspended stripline RF MEMS tunable filter with bandwidth control," *IEEE Trans. Microw. Theory Tech.*, vol. 59, no. 10, pp. 2469-2476, Oct. 2011.
- [3] J.-X. Chen, L.-H. Zhou, H. Tang, Z.-H. Bao, and Q. Xue, "Theory and experiment of wideband tunable forced-mode ring resonator," *IET Microw. Antennas Propag.*, vol. 7, no. 5, pp. 332-337, Apr. 2013.
- [4] C. H. Kim and K. Chang, "Ring resonator bandpass filter with switchable bandwidth using stepped-impedance stubs," *IEEE Trans. Microw. Theory Tech.*, vol. 58, no. 12, pp. 3936-3944, Dec. 2010.
- [5] J.-S. Hong, *Microstrip Filters for RF/Microwave Applications*, 2nd ed. Hoboken, NJ: J. Wiley & Sons, 2011.